



The associated tasks of integrating the required electronic equipment, such as interrogator, mini-PC, or power supply into the airframe will also be discussed, followed by a description of the data transfer from the rotating to the non-rotating frame. Real-time health monitoring of the rotor blades is done by integrating the Vehicle Health Monitoring (HT-VMU) vibration monitoring unit on the H135 to capture data not only from the fibre optic sensors, but also from other sensors and on-board avionics. The paper concludes by summarising the key challenges of systems integration, such as the integration of the HT-VMU with the fibre-optic system, synchronisation of the data streams and the data transmission using WiFi to stream strain and blade shape during operation for health monitoring, balancing the hub support cap assembly, and the attachment of the fibre optic sensors to the surface of the rotor blade.

## 2. MATHEMATICAL BASELINE MODELS

For health monitoring of a rotor blade a mathematical baseline model is essential in order to predict its aeroelastic behaviour. Any deviation from normal structural dynamics indicate damage. Within this project a fluid-structure interaction (FSI) framework was developed, that consists of computational fluid dynamics (CFD) coupled with finite element analysis (FEA) to provide steady state structural deformations along the rotor blade for different azimuth and pitch angles. Based on this output a stochastic model was developed to surrogate the computationally expensive FSI model.

The developed CFD model predicts the forces and moments on the main rotor blades at 1000 ft hover assuming the absence of any ambient wind conditions. Figure 2 shows the predicted downwash of the helicopter in hover. The blade pitch and azimuth angles were varied in each simulation to define different blade operating conditions.

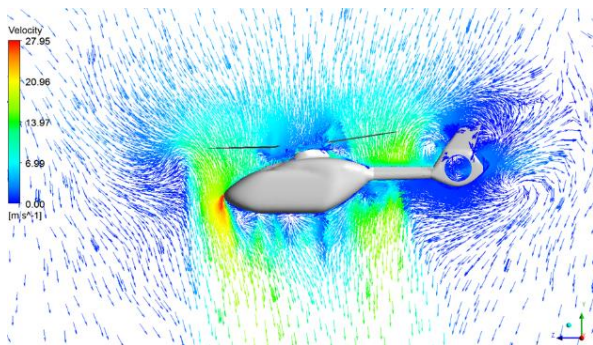


Figure 2: Downwash in hover condition at 1000 ft

In the CFD model, the steady state Reynolds Averaged Navier-Stokes (NS) equations were solved in a domain encompassing the helicopter body and the main rotor. The domain extended approx. 10 times the rotor diameter distance around the helicopter, and consisted of two regions – one annular region surrounding only the rotor blades and the other region surrounding both the annular region and the helicopter body. The NS equations were solved in the Moving Reference Frame (MRF) in the rotor region to model the effect of blade motion implicitly [1]. The surfaces of the domain boundary were modelled as farfield, while the rotor and the helicopter body surfaces were modelled as smooth no-slip walls. A commercial CFD solver, Ansys Fluent (v17.2) [1], was used to solve the NS equation over the discretized domain. The domain was discretized into an unstructured mesh with 22.5 million cells (prism, tetra and quad cells), with wall  $Y^+$  values less than 80. The NS equations were discretized over each cell in the unstructured mesh. The two equation  $k-\omega$  SST model by Menter was used for modelling the turbulence [2]. The simulations were iteratively solved until convergence was achieved. In post-processing, the pressure and shear forces on the blade surface were used to compute the forces and moments on the nodal points for the FSI simulations. Results obtained from CFD were compared with GPU based aeroelastic modelling that utilised the unsteady vortex lattice method [3].

The finite element analysis (FEA) model of the H135 bearingless main rotor blade was constructed using standard finite-element-modelling techniques in Nastran. Figure 3 shows that the complex structure of the rotor blade is modelled by using multiple beams, which consists of a primary one-dimensional stick for the flexbeam and the blade aerofoil section, and a secondary stick parallel to the flexbeam representing the pitch control cuff.

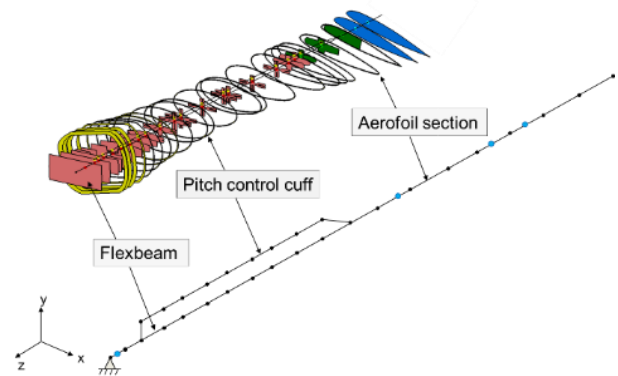


Figure 3: Structural main rotor blade model

Structural loading tests as well as impact hammer tests (IHT) were done to assess the performance of the FEA model against a real rotor blade. Results yielded a 10 % agreement between natural frequencies of the FEA model and test data. Additionally, the obtained experimental results were used to minimise the error between the predicted and experimentally determined modal properties with the use of an indirect finite element model updating procedure.

Finally, the FSI couples the aerodynamic loading to the FEA model to obtain steady state structural deformations along the rotor. This is also the input to the stochastic model, which is a three-dimensional vector specifying blade pitch angle, blade azimuth angle and a position on the blade (the distance from the rotor axis along a defined line on the blade). The output<sup>1</sup> is the predicted blade deformation at that point measured by three translation components and three for the rotation. Figure 4 shows a typical output plot for a set of points on the blade.

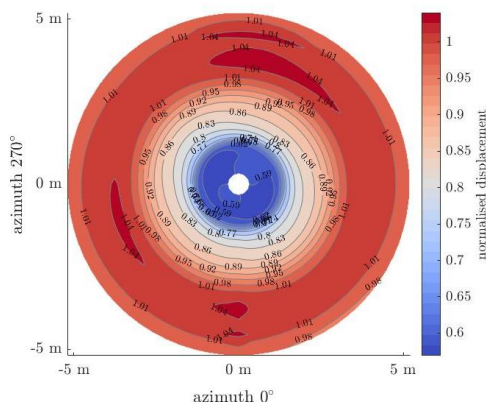


Figure 4: Typical output of stochastic model

Different types of model were investigated, including linear models, interpolation methods and Gaussian process regression. These could all be classed as ‘machine learning’ whereby a set of ‘training data’ (inputs plus corresponding outputs from the FSI model) was used as the basis on which to predict blade deformation for any input vector with components within the ranges under consideration, viz. pitch angle 8-12 degrees, azimuth angle 0-360 degrees, any point along the blade. An interpolation method was chosen because it was judged to perform best in terms of predictive accuracy, speed and computational cost. Since the stochastic model uses interpolation, its output matches the results from the FSI model

<sup>1</sup> The output from the model is deterministic, but the model is called ‘stochastic’ partly for historical reasons, plus the fact that the output is treated as being a realisation of a stochastic process in the real world.

when the training data is used as input. No separate validation data from the FSI model was available and it would have been expensive to produce, so the overall accuracy for any input vector was judged using cross-validation. It was estimated that the difference between the stochastic and FSI model predictions would normally be less than 1% of R, where R is the predicted range of output values over all possible inputs. For one of the translations the upper limit was, however, 2% of R. The stochastic model runs in negligible time on a typical laptop computer. For example, for given pitch and azimuth angles, it takes about 10 milliseconds to calculate the six displacements at 120 points along the blade.

Apart from developing a methodology that is suitable for real-time rotor blade dynamic analysis, an in-house tool was developed in MATLAB/Simulink to predict aeroelastic behavior. This couples the FEA model with a dynamic inflow model and blade element analysis to calculate the local angles of attack at each time step. This aeroelastic tool forms the root for several activities, such as fibre-optic sensor placement mapping, or reproducing the final tied down test in a simulation environment by exciting the rotor blade dynamics due to a given pilot input.

### 3. FIBRE OPTIC INSTRUMENTATION SYSTEM

Optical fibre based sensing approaches have been adopted for this application as they offer a number of key benefits, including their flexibility, low weight, electromagnetic immunity, small dimensions (~0.2 mm diameter), no requirement for electrical connection to the sensing elements and the ability to multiplex a number of sensors within a single length of optical fibre. In addition, optical fibres can be embedded within fibre reinforced composites during fabrication, or, alternatively, can be surface-mounted to facilitate retrofitting [4] [5] [6]. Two optical fibre sensing technologies will be trialled: optical fibre Bragg gratings (FBGs) and direct fibre optic shape sensing (DFOSS).

FBGs represent a mature sensing technology that is commercially available. An FBG is a method for labelling a short section of optical fibre (of length typically 0.5 – 5 mm) such that it can be uniquely interrogated to monitor local environmental parameters such as strain and temperature [7]. The label takes the form of a grating structure that is created within the core of the optical fibre by exposure of the fibre to a spatially modulated UV

laser beam. The grating acts as a wavelength selective mirror, reflecting a single wavelength of light back along the optical fibre. Perturbation of the grating by strain or temperature results in a change in the reflected wavelength, the measurement of which formed the basis of the sensing approach. It is possible to multiplex a number of such sensors within a single optical fibre by fabricating each FBG such that in their quiescent states they each reflect different wavelengths. Typical commercially available sensor interrogation units (which can be flight-certified) are capable of performing measurements of strain and temperature with resolutions of  $1 \mu\epsilon$  and  $0.1 \text{ K}$ , respectively, in 4 - 16 fibres, with tens of sensors per fibre, at data rates up to 100 kHz (typically of order 1 kHz). In this application, arrays of FBG strain sensors, attached to the upper and lower surface of the blade, will be used to measure the vibration mode shapes indirectly, where the data has to be combined with a model of the blade to determine the shape from the measured strain [8].

DFOSS allows changes in the fibre path, and thus changes in the shape of the structure to which the fibre is attached, to be followed in three dimensions. A key advantage of DFOSS is that the shape is determined directly within the sensing fibre, removing the dependence on strain transfer from the structure and thus the requirement for a model of the structure. Simple surface mounting of the sensing fibre, for example using adhesive tape, is, in principle, sufficient. The DFOSS approach proposed here [9] is based on Fibre Segment Interferometry, an approach pioneered at Cranfield University [10] [11], which employs a simple, cost-effective and robust interrogation system exploiting well-proven telecoms laser diodes, detectors and optical fibre components to offer highly sensitive high-speed dynamic curvature measurements. The approach relies on differential measurements of strain in fibre segments formed in the cores of a multi-core optical fibre, with the segments bounded by low reflectivity, broad bandwidth FBGs.

#### 4. ON-BOARD SYSTEM

There are two main components within the Helitune on-board system: the RT-TipTrak blade tracking camera and the HT-VMU Vibration Monitoring Unit, plus additional supporting sensors.

The RT-TipTrak camera uses a line scan CCD (a single line of pixels) to capture an image of the rotor blade tip as it passes through the field of view. Using edge detection algorithms and geometry information about the aircraft, a measurement of blade height and lead/lag can be made for each blade and for each revolution of the rotor. For the purposes of the flight trials in the current study, the

camera was mounted on the H135 to the central pillar behind the pilot in the cockpit and aimed through the windscreen at a clock angle of approximately 1 o'clock.

The HT-VMU is based on the existing Helitune RT-6 VMU that provides Rotor Track & Balance functions and data recording but extends these features with additional data capture and processing capabilities.

The system records lateral vibration data for the H135 main rotor from an accelerometer mounted on the transmission, and vertical vibration from an accelerometer mounted beneath the floor in the cockpit. Tail rotor radial vibration is recorded from an accelerometer mounted on the hub of the Fenestron. The system also records a 1/rev signal from the main and tail rotors using magnetic pick-up units (MPUs) in order to determine the position of the rotor for signal processing and blade tracking. The HT-VMU is able to calculate and log 1R (main rotor vibration) and 1T (tail rotor vibration) measurements, in addition to capturing time domain vibration data in parallel for offline analysis.

The HT-VMU features ARINC 429 receivers in order to log aircraft parameters from the Air Data Computer, including altitude, air speed, heading etc. A key challenge in aircraft integration was locating a suitable interface point to obtain an ARINC data feed. For the initial flight trials an H135 aircraft with the Helionix avionics system was used and a suitable tapping point was found on the Traffic Advisory System in the rear avionics shelf.



Figure 5: RT-TipTrak (top) and HT-VMU (bottom) mounted to the central pillar on the H135.

In order to mitigate against the possibility of not locating a suitable ARINC data feed on future test aircraft or any difficulties in decoding the messages, two other additional sensors have been included in the system. A GPS antenna is connected to the HT-VMU to provide location, altitude and ground speed information, and a 6-axis sensor is connected to provide orientation data.

The final interface element with the HT-VMU is for the fibre-optic data feed from the BladeSense system. This data is transmitted from the WiFi antenna on the BladeSense assembly to a remote WiFi antenna mast (Figure 6). The signal is then routed to a laptop and then back to the HT-VMU in order to capture the data synchronously with all of the other data streams. There were a number of different options for the interface but eventually ethernet was chosen in order to achieve the required data rates and integrity of data transmission.

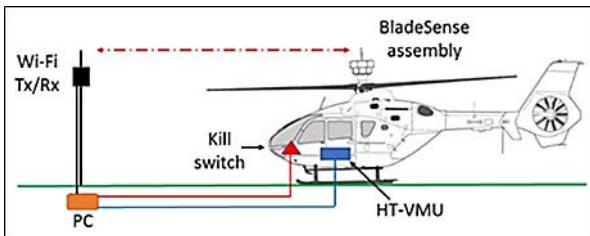


Figure 6: Schematic showing the connections between the instrumentation PC and the Helitune HT-VMU.

The HT-VMU was also mounted to the central pillar behind the pilot in the cockpit for the flight trials and 28V aircraft power was obtained from the breaker panel in the rear of the aircraft.

## 5. SYSTEM INTEGRATION

As discussed in Section 3, both strain and shape sensing instrumentation systems were fabricated during this project. Both systems use identical Li-ion battery technology, a mini-PC and a power management control system. The mini-PC is remotely controlled via a stationary PC using Wi-Fi. The strain sensing system uses a commercially supplied compact interrogator whereas the shape sensing interrogator was designed in-house at Cranfield University. The assemblies and components for the system were selected according to the following criteria: low mass, compactness, low power dissipation and resistance to shock and vibration in accordance with aerospace standards DO-160G [12]. The electronic modules were packaged in an outer assembly which was designed by Airbus Helicopters UK. This assembly is attached to the

rotor hub cap support via an interface ring and a CATIA model of the arrangement is shown in Figures 7 and 8. The Li-ion batteries are located in the base of the hub cap support. The Wi-Fi antenna is attached to the top plate of the assembly on the axis of rotation. Both shape and strain assemblies weigh approximately 10 Kg.

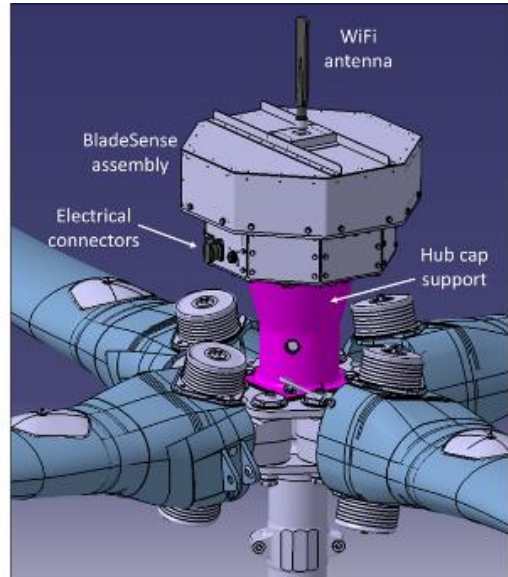


Figure 7. BladeSense assembly attached to hub cap support.

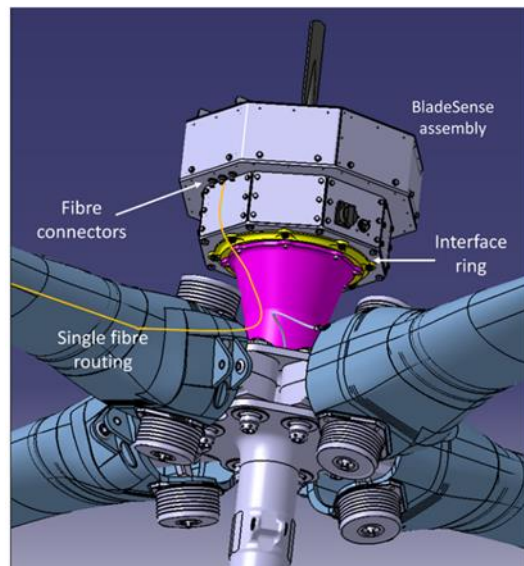


Figure 8. Under side view of the assembly, showing a typical routing of one fibre from the blade to a fibre connector.

Internal components have been located to minimize mechanical imbalance of the internal assemblies. Three fibre optic sensor cables are attached to two opposing blades and are connected to the BladeSense assembly via six

fibre optic connectors. Three of these optical connectors are shown in Figure 8. The WiFi antenna used has an omni-directional radiation pattern and can operate on both 2.4/ 5.0 GHz frequencies. The internal PC Wi-Fi card provides the RF signal. Maximum data rate is  $54 \text{ Mbs}^{-1}$  at a power of  $\sim 10 \text{ dBm}$ .

A prototype assembly of the strain sensing variant has been fabricated to assess the basic system functionality. This is shown in Figure 9. The hub cap support assembly was attached to a circular plate (potter's wheel) which can rotate the assembly from 0 to  $\sim 395 \text{ r.p.m.}$  which is the operational speed of the H135 helicopter rotor. Two FBG sensors were adhered to a weighted steel rod and these measured the varying tensile strain in the rod as the rotation speed was increased. The strain data streamed from several trials was received via a stationary instrumentation PC over a distance of 55 m. The stationary PC controlled the mini-PC in the prototype in remote mode.

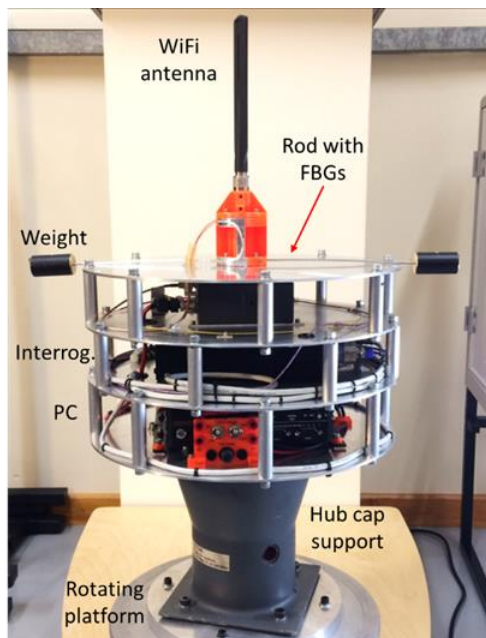


Figure 9. Early prototype strain sensing interrogator where the strain induced in a weighted steel rod was determined.

In order to mount the BladeSense assembly on the aircraft rotor it is critical that it is balanced in order to minimise any vibrational loads transferred to the rotor head.

The prototype BladeSense assembly was statically balanced by mounting it on bearings with the rotational axis horizontal so that any off-axis centre of mass would cause it to rotate. Balance weights were applied using bolts to one of the structural pillars to reduce any rotation as much as possible.

To further reduce any potential vibration, a dynamic

balance was conducted by mounting the hub support cap and prototype BladeSense assembly to a potter's wheel, as this was a convenient drive mechanism for the loads and rotational speeds required. A Helitune RT-5 JS+ Rotor Track and Balance System was used with Optical Pick-up (for 1/rev signal) and axial and radial accelerometers fitted to the structure of the potter's wheel.

An initial dynamic balance recording was made on the drive mechanism without the BladeSense assembly. This proved to be sufficiently well balanced in itself, giving a reading of approximately 0.01 inches per second (ips).

The prototype BladeSense assembly was then attached to the drive mechanism and initial balance data was recorded with the rotational speed confirmed at 396 RPM, in line with the H135 nominal rotor speed (nR). The radial balance was 0.078 ips. Trial weight adjustments were carried out to assist in obtaining the adjustment offset and sensitivity required by the RT-5 JS+ system. A final weight adjustment of 20 g was applied to the top plate of the device based on the balance point move vectors obtained from the trial adjustments. The result was a residual balance figure of 0.031 ips in the lateral (radial) plane and 0.014 ips in the vertical (axial) plane. A further round of balancing is envisioned once the BladeSense assembly has been installed on the aircraft, which will make use of the on-board accelerometers and normal rotor balancing adjustment weights.

## 6. CONCLUSIONS & FURTHER WORK

The technology to measure in-flight blade dynamics aims to overcome existing limitations in design, operation and maintenance of helicopter blades. This paper provides the reader with a summary of key activities in the BladeSense project. The engineering approach and design challenges in areas such as modelling and simulation, instrumentation development and ground testing are presented and discussed. These range from the use of computational aerodynamics and structural modelling to predict blade dynamics to the development of direct fibre optic shape sensing that allows measurements above 1kHz over numerous positions on the blade. The development of the prototype onboard system that overcomes the challenge of transferring data between the rotating main rotor to the fixed fuselage frames is also discussed.

For the remainder of this project a number of key activities need to be carried out. The first is to develop the attachment process of the optical fibres to both the top and underside of the blades. The optical fibre diameter is  $\sim 250 \mu\text{m}$ . It is

expected that the fibres will be adhered to the full length of the blade and be located beneath the erosion protective polyurethane tape (thickness ~ 500  $\mu\text{m}$ ) which is located on the leading edge of the blade. Another activity is to undertake an open-air Wi-Fi range trial at representative antenna heights to confirm the maximum achievable range of the system. This is followed by the activity to integrate the HT-VMU with the fibre optic instrumentation PC so that shape and strain data is streamed to the HT-VMU. The HT-VMU will provide a timestamped signal so allowing the RT-TipTrak data to be synchronised with the optical shape and strain data. At the end of the project a tie down test with a H135 helicopter will be used to demonstrate the capability of the developed technology. Data collected from this experiment will be analysed and assessed by comparing with the results obtained from the mathematical baseline models.

## 7. REFERENCES

- [1] Ansys Fluent User's Guide v17.2, Ansys, 2016.
- [2] F.R. Menter, "Two-equation eddy-viscosity turbulence models for engineering applications", American Institute of Aeronautics and Astronautics Journal, Vol. 32, No. 8, 1994, pp. 1598-1605.
- [3] D. Fleischmann, M. Lone, S. Weber, A. Sharma, "Fast Computational Aeroelastic Analysis of Helicopter Rotor Blades", 2018 AIAA Aerospace Sciences Meeting, AIAA SciTech Forum, (AIAA 2018-1044).
- [4] N. Lawson, R. Correia, S. W. James, R.P.Tatam, et al., "Development and application of optical fibre strain and pressure sensors for in-flight measurements", Meas. Science and Tech., 27, Art. 104001, (2016).
- [5] S. J. Buggy, S.W. James, S. Staines, R. P. Tatam, et al., "Railway track component condition monitoring using optical fibre Bragg grating sensors", Meas. Science and Tech., 27, Art. 055201, (2016).
- [6] R. M. Groves, E. Chehura, W. Li, R.P.Tatam, et al., "Surface strain measurement: a comparison of speckle shearing interferometry and optical fibre Bragg gratings with resistance foil strain gauges", Meas. Science and Tech., 18, pp. 1175-1184, (2007).
- [7] A. Cusano, A. Cutolo and J. Albert, "Fiber Bragg Grating Sensors: Recent Advancements, Industrial Applications and Market Exploitation" Bentham Science Publishers (2018).
- [8] M.J. Nicolas, R. W. Sullivan, W. L. Richards, "Large Scale Applications Using FBG Sensors: Determination of In-Flight Loads and Shape of a Composite Aircraft Wing" Aerospace 3, 18 (2016).
- [9] T. Kissinger, E. Chehura., S.E. Staines, S.W. James, R.P. Tatam, "Dynamic fiber-optic shape sensing using fiber segment interferometry," J. Lightwave Technol., 36, 917-925 (2018).
- [10] T. Kissinger, T.O.H. Charrett, R.P. Tatam, "Range-resolved interferometric signalprocessing using sinusoidal optical frequency modulation," Opt. Express 23, 9415-9431 (2015).
- [11] T. Kissinger, R. Correia, T.O.H. Charrett, S.W. James, R.P. Tatam, "Fiber segment interferometry for dynamic strain measurements," J. Lightwave Technol., 34, 4620-4626 (2016).
- [12] Radio Technical Commission for Aeronautics (RTCA) DO-160 G: Environmental Conditions and Test Procedures for Airborne Equipment.

---

### Copyright Statement

*The authors confirm that they, and/or their company or organization, hold copyright on all of the original material included in this paper. The authors also confirm that they have obtained permission, from the copyright holder of any third party material included in this paper, to publish it as part of their paper. The authors confirm that they give permission, or have obtained permission from the copyright holder of this paper, for the publication and distribution of this paper as part of the ERF proceedings or as individual offprints from the proceedings and for inclusion in a freely accessible web-based repository.*

# Bladesense – a novel approach for measuring dynamic helicopter rotor blade deformation

Weber, Simone

2018-12-31

Attribution 4.0 International

---

Weber S, Southgate D, Mullaney K, James S, Rutherford R, Sharma A, Lone M, Kissinger T, Chehura E, Staines S, Pekmezci H, Fragonara LZ, Petrunin I, Williams D, Moulitsas I, Cooke A, Lawson N, Rosales W, Tatam R, Morrish P, Fairhurst M, Atack R, Bailey G & Morley S.

Bladesense – a novel approach for measuring dynamic helicopter rotor blade deformation. In: 44th European Rotorcraft Forum (ERF 2018), Delft, 18-21 September 2018

<https://www.erf2018.org/>

*Downloaded from CERES Research Repository, Cranfield University*